Dariz *et al. Heritage Science* (2022) 10:37
https://doi.org/10.1186/s40494-022-00678-6

Heritage Science

RESEARCH ARTICLE Open Access

Beautiful Pietàs in South Tyrol (Northern Italy): local or imported works of art?

Petra Dariz[1], Ulrich G. Wortmann[2], Jochen Vogl[3] and Thomas Schmid[3*]

Abstract

The study, dedicated to Beautiful Pietàs conserved in South Tyrol (Northern Italy), aims to establish, for the first time, a connection between Austroalpine raw materials and the high-fired gypsum mortars constituting the Gothic figure groups in question. The origin and chronology of this stylistically and qualitatively differing ensemble have been subject of art historical debate for nearly a century. The discourse is dominated by three main hypotheses: itinerary of an Austrian artist versus itinerary of the work of art created in an artist's workshop in Austria versus itinerary of the stylistic vocabulary via graphical or three-dimensional models. The comparison of the $\delta^{34}S$ values and the $^{87}Sr/^{86}Sr$ ratios of the gypsum mortars and Austroalpine sulphate deposits (in a compilation of own reference samples and literature data) points to the exploitation of sediments in the Salzkammergut and possibly also in the evaporite district of the Eastern Calcareous Alps, thus evidencing the import of the sculptures and not the activities of local South Tyrolean or itinerant artists. Two geochronological units are distinguishable: The Pietà in the Church St. Martin in Göflan can be assigned to Upper Permian raw material, whereas the metrologically consistent sculptures in the Church of Our Lady of the Benedictine Abbey Marienberg and in the Chapel St. Ann in Mölten correlate with deposits of the Early Triassic (or the Lower-Middle Triassic transition). The medieval gypsum mortars also differ in their mineralogical characteristics, i.e. in their geologically related minor components, as in the first case, characterised by a significant proportion of primary anhydrite, natural carbonate impurities mainly consist of calcite (partly converted to lime-lump-like aggregates), whereas in the second group dolomite (or rather its hydration products after pyrometamorphic decomposition) predominates, accompanied by celestine, quartz and potassium feldspar. The Pietà in the Cathedral Maria Himmelfahrt in Bozen turned out to be made of Breitenbrunn calcareous sandstone (Leitha Mountains, Burgenland, Austria), which is why the sample is not considered in the geochemical analysis.

Keywords: High-fired gypsum mortar, Evaporite, Upper Permian, Early Triassic, Eastern Alps, Sulphur isotope, Strontium isotope, Polarised light microscopy, Raman microspectroscopy, Breitenbrunn calcareous sandstone

*Correspondence: thomas.schmid@bam.de
[3] Department of Analytical Chemistry, Reference Materials, Federal Institute for Materials Research and Testing, 12489 Berlin, Germany
Full list of author information is available at the end of the article

Graphical Abstract

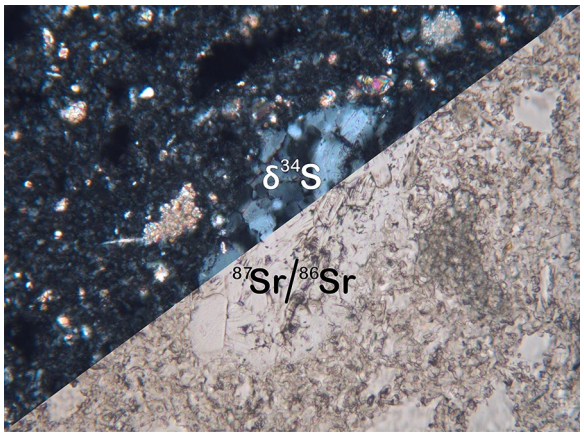

Introduction

For nearly a century the phenomenon of itinerant artists has been a subject of debate in the art historical research field of the Gothic Beautiful Madonnas and Pietàs. The spread of such figure groups in Central Europe and the Apennines around 1400 is explained by the activities of Bohemian, Viennese, Salzburg or Hungarian "Wandermeister" [1–5], possibly appointees [6, 7], economic migrants [8], etc. In the art historical discourse, the itinerary of the artist is opposed to the itinerary of the work of art in terms of large-scale production of Madonnas and Pietàs intended for the export [1, 9–26]. Furthermore, also their creation in local workshops or artists' colonies, be it under the direct influence of itinerant artists or due to the transfer and appropriation of the stylistic vocabulary through the medium of pattern books and independent prints or three-dimensional models, is discussed [2, 7, 14, 19, 23, 27–29].

The study at hand is dedicated to an ensemble of Beautiful Pietàs conserved in South Tyrol (Northern Italy), whose reception history mirrors the mentioned central lines of the art historical argumentation. By way of example, the Pietà exhibited in the Cathedral Maria Himmelfahrt in Bozen is attributed to a Salzburg [9, 17] or Carinthian [30, 31] workshop, to a nameless itinerant Bohemian artist [4] or to Hans of Judenburg (Styria, Austria), who was responsible for the design and the creation of the high altar in the parish church of Bozen in the early 1420s [32, 33]. The delicate figure group is classified as model or inspiration for local creations, even if realised in modified proportions, postures and emotional expressions: The three Pietàs in the Church of Our Lady of the Benedictine Abbey Marienberg above Burgeis, the Chapel St. Ann in Mölten and the pilgrimage church Our Lady of the Seven Dolours in Cavalese (Fiemme Valley, Trentino) bear substantial resemblance, for which reason Eva-Maria Kreuzer-Eccel [33, 34] favours a common provenance in the form of a local workshop. In contrast, Carl Müller [9] hypothesises an import from Salzburg, whereas Louis Springer [30, 31] and Nicolò Rasmo [35, 36] subsume the three figure groups as the oeuvre of an itinerant Salzburg artist. Similarly, the Pietà in the Church St. Martin in Göflan is graded by Carl Müller [9] as coarsely sculpted and thus local work; in contrast, Louis Springer [30] relates the figure group as a primitively simplified piece to the workshop of the master of the Virgin Mary in the pilgrimage church of Our Lady on the Gmain in Großgmain (State of Salzburg, Austria).

The art historical hypotheses and lines of reasoning formed in the course of the twentieth century are based primarily upon stylistic observations (elaboration of distinct details such as drapery, side parts and corner-pieces of the throne bench, "Dreihändespiel", etc.) and historical investigations, not unaffected by the respective contemporary body of thought [37]. The present study aims to resume the scholarly discussion on the provenance of four exemplarily selected Beautiful Pietàs by making use of traces of the raw material embodied in the high-fired gypsum mortars constituting the figure groups in question, as little variations in the execution of the basic shape and related details do not allow to unambiguously deduce the source area. Overarching analytical methodology is the petrographic study of Austroalpine gypsum deposits and medieval mortars by a combination of microscopic and spectroscopic techniques. The main emphasis of these observations is on geologically related minor components of the sample material. As sedimentary or evaporite deposit, gypsum $CaSO_4 \cdot 2H_2O$ is often

associated with carbonate minerals (calcite $CaCO_3$, magnesite $MgCO_3$, dolomite $CaMg(CO_3)_2$), sulphates (anhydrite $CaSO_4$, celestine $SrSO_4$), quartz SiO_2, feldspars as well as phyllosilicates like clay minerals or members of the mica and the chlorite group [38, 39]. Mineralogy and amount of such natural impurities vary locally. Hendrik Visser and Albrecht Wolter mention the possibility to differentiate gypsum beds and hence gypsum mortars from Schleswig–Holstein and the Harz in Northern Germany on the basis of the presence of accompanying magnesite or dolomite, respectively [40], since high-fired gypsum mortars consist mainly of the rehydrated binder, i.e. in the majority of cases no mineral aggregates were added [41–43].

Beyond that, the geochemical comparison of sulphur and strontium isotopic signatures is included in the research work as additional indicator of origin, as the variability between alpine gypsum beds only regarding their mineral assemblage is too restricted for a documentation of provenance. In geological and environmental studies, the $^{87}Sr/^{86}Sr$ ratio has proved valuable—along with $\delta^{34}S$ and $\delta^{18}O$—in determining the depositional age of calcium sulphate layers, since significant amounts of strontium can be incorporated in the crystal lattice of gypsum and anhydrite in substitution for calcium ions. Apart from that, most of the mainly Permian and Triassic evaporitic sediments in question contain accessory celestine, which, according to the literature [44, 45], survives the typical medieval calcination temperatures of about 900 °C without structural alterations.

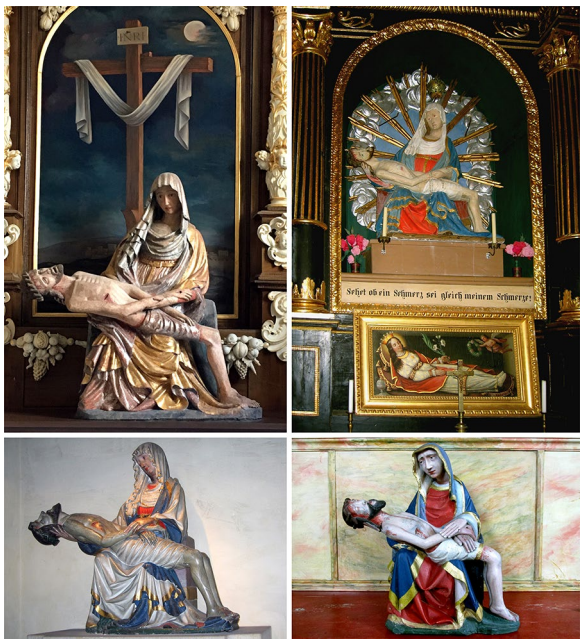

Fig. 1 Pietà in the Church of Our Lady of the Benedictine Abbey Marienberg (height 135 cm × width 100 cm × depth 45 cm) (top, left), Pietà in the Chapel St. Ann in Mölten (105 cm × 80 cm × 35 cm) (right), Pietà in the Cathedral Maria Himmelfahrt in Bozen (85 cm × 95 cm × 35 cm) (bottom, left) and Pietà in the Church St. Martin in Göflan (60 cm × 40 cm × 25 cm) (right)

Materials and methods

Samples

Samples of the high-fired gypsum mortars were taken from the Beautiful Pietàs in the Cathedral Maria Himmelfahrt in Bozen, the Church of Our Lady of the Benedictine Abbey Marienberg above Burgeis, the Chapel St. Ann in Mölten and the Church St. Martin in Göflan (see Fig. 1). Reference samples of South Tyrolean and Austrian gypsum deposits were collected in the course of geological field work and provided by the Natural History Museum (Vienna, Austria), Geologische Bundesanstalt (Vienna, Austria) and the Museum für Naturkunde (Berlin, Germany).

Polarised light microscopy

The gypsum mortars and stones were prepared for analysis in a specialised laboratory by embedding in epoxy resin under vacuum and manufacturing polished thin sections (30 µm thickness), which were studied under polarising light microscopes (Leica Microsystems Laborlux equipped with ProgRes SpeedXT3 and Zeiss AxioScope.A1 MAT equipped with AxioCam MRc) in transmitted polarised light.

Raman microspectroscopy

Identifications of mineral phases by polarised light microscopy were complemented by Raman microspectroscopic single-point measurements or two-dimensional mapping experiments. The resulting spectra were assigned by comparison with reference data from the RRUFF database library [46]. Thin-sectional samples were analysed by employing a LabRam HR 800 Raman microscopy system (Horiba JobinYvon) equipped with a BX41 microscope (Olympus). A 532-nm green laser beam was focused by a 50×/NA = 0.75 objective lens (with NA denoting the numerical aperture) onto the sample surface, and the backscattered light collected by the same lens—after passing two 532-nm edge filters—was fed into a dispersive spectrograph with a 1800-mm^{-1} grating and a liquid-N_2 cooled (− 130 °C operating temperature) charge coupled device (CCD) detector (Symphony, Horiba Jobin Yvon). See Ref. [47] for further details. The Raman microspectroscopic maps shown in Fig. 3 and 7 were acquired by focusing 15 mW laser power (50% of the maximum available power) onto a thin-section and mapping the sample by

movement through the focal volume with a step size of 1 µm × 1 µm and acquisition of a Raman spectrum (average of 3 acquisitions of 5 s each or 3 × 5 s, respectively) ranging from 860 cm^{-1} to 1330 cm^{-1} at every measurement spot with a spectral resolution of approx. 0.4 cm^{-1} per CCD pixel. Raman phase distribution maps were calculated by plotting baseline-corrected peak heights of the following marker bands as intensities of false colours: 984 cm^{-1} (hexahydrite, yellow), 1008 cm^{-1} (gypsum, green), 1017 cm^{-1} (anhydrite, red), 1086 cm^{-1} (calcite, blue), and 1101 cm^{-1} (high magnesian calcite, cyan; evaluation of the falling edge of a broad band). With the same instrument, using a Peltier-cooled CCD detector (Syncerity, Horiba Jobin Yvon; − 60 °C), 20 Raman maps each of three powdered gypsum stone samples having the same pixel sizes and consisting of 70 × 70 = 4900 spectra (2 × 0.5 s acquisition time per spectrum) were acquired with the aim of detecting mineral phases also at trace levels, below the detection limit of powder X-ray diffraction analysis (see Additional file 2: Figs. S4–S8 in the Results and Discussion).

The Raman maps shown as Additional file 2: Figs. S9 and S10 in the Results and Discussion were acquired using a table-top Jasco NRS-4100 Raman microscopy system coupled to an upright Olympus microscope, equipped with notch filters and a CCD detector (Andor; − 60 °C). A diode-pumped solid-state laser with a wavelength of 532 nm was focused by a 100 × / NA = 0.9-objective lens onto the sample surface. In order to avoid sample damage, the laser power was attenuated to 10% of the original power, or to 0.6 mW respectively, by inserting neutral density filters into the beam path. The collected backscattered light (acquisition time: 2 × 2 s) was dispersed by a spectrometer grating having 1800 lines per mm, resulting in spectra ranging from 50 cm^{-1} to 1995 cm^{-1} with a resolution of around 1.2 cm^{-1} per CCD pixel. The analysed marker bands and false colours are: 350 cm^{-1} (pyrite, yellow), 451 cm^{-1} (rutile, white), 509 cm^{-1} (albite, cyan), 511 cm^{-1} (plagioclase, cyan), 686 cm^{-1} (chlorite/phlogopite, magenta), 706 cm^{-1} (muscovite, brown), 965 cm^{-1} (apatite, magenta), 1000 cm^{-1} (celestine, blue), 1008 cm^{-1} (gypsum, green), 1302 cm^{-1} (haematite, red).

Sulphur isotope analyses

Sulphur isotope ratios were determined at the Geobiology Stable Isotope Laboratory (GIL) at the Department of Earth Sciences, University of Toronto (Canada). Tin capsules enclosing approximately 160 µg of powdered and homogenised sample were introduced into a Eurovector Elemental Analyzer (EA3000 series) and flash combusted under oxygen atmosphere. The resulting sulphur dioxide gas was introduced via an open split interface (Conflo III) to a continuous-flow isotope ratio mass spectrometer (CF-IRMS, Finnigan MAT 253). The measured sulphur isotope ratios were calibrated against NBS 127 ($\delta^{34}S = +21.12‰$), IAEA-SO-5 ($\delta^{34}S = +0.49‰$) and IAEA-SO-6 ($\delta^{34}S = -34.05‰$) distributed by the International Atomic Energy Agency; an in-house barium sulphate $BaSO_4$ standard ($\delta^{34}S = +8.9‰$) was used to monitor for instrument drift. Precision was measured by the repeated analysis ($n \geq 10$) of NBS 127 and the GIL inhouse standard, which yields a 1-σ error of 0.11‰ and 0.28‰ respectively. All values are reported as $\delta^{34}S$ relative to the Vienna-Canyon Diablo Troilite (V-CDT) standard using the conventional delta notation [48].

Strontium isotope and mass fraction analyses

Strontium isotope analyses were carried out in a metal-free cleanroom at the Federal Institute for Materials Research and Testing, Department of Analytical Chemistry; Reference Materials, Division 1.1 Inorganic Trace Analysis, in Berlin (Germany) by using ultrapure reagents. For extraction over a period of 7 to 10 days 10 mL of Milli-Q water was added to 10 to 20 mg of crushed sample material, sometimes supporting the release of strontium ions by gentle heating at 80 °C on a hotplate. Thereafter, the sample solution was centrifuged to separate very few remaining and mostly coloured particles.

For quantitative strontium analyses by inductively coupled plasma mass spectrometry (ICP-MS) 10 to 100 µL of the centrifugate were diluted to a nominal mass fraction of 1 to 200 µg/kg to match the dynamic ranges of the instruments. External calibration was carried out with or without internal standardisation, depending on the final matrix dilution. The relative expanded measurement uncertainty was assessed to be 20%, including contributions from sample preparation, dilution, repeatability of the measurements and calibration standards.

A subsample of the centrifugate containing approximately 5 µg strontium was further prepared for strontium isotope ratio analyses by thermal ionisation mass spectrometry (TIMS): The subsample was evaporated to dryness and redissolved in nitric acid, before performing a separation of strontium from matrix on Eichrom Sr Spec resin (Triskem International, Bruz, France). The obtained strontium fraction was repeatedly evaporated to dryness and redissolved to yield a solution with a final strontium mass fraction of 100 ng/µL. After loading 1 µL of this solution on a rhenium single filament together with a tantalum pentachloride $TaCl_5$ activator, the filament was mounted on a sample turret, which was inserted into a Sector 45 type multi-collector TIMS instrument (Micromass, Manchester, United Kingdom). The instrument was run in dynamic multi-collection mode with automated measurement procedures, yielding

conventional $^{87}Sr/^{86}Sr$ isotope ratios; this includes corrections for the ^{87}Rb interference on ^{87}Sr, the correction of the instrumental isotope fractionation via the fixed value of $^{86}Sr/^{88}Sr = 0.1194$ using the power law and finally a normalisation of the $^{87}Sr/^{86}Sr$ reference value for the certified NIST SRM 987 strontium carbonate isotopic standard (National Institute of Standard and Technology, Gaithersburg, United States) [49, 50]. The typical repeatability for 200 replicates within one filament, expressed as twice the standard error (2SE), was 0.000012, the reproducibility, as obtained on 8 independently prepared samples measured 31 times in total, was 0.000004. For quality control, NIST SRM 987 and NASS-6 Seawater reference material for trace metals (National Research Council of Canada, Ottawa, Canada) were processed the same way as the gypsum samples except for the extraction. The obtained $^{87}Sr/^{86}Sr$ isotope ratios agreed well with the reference values within their uncertainties. Based on the validation and quality control data, an expanded measurement uncertainty U (k = 2) of 0.000024 was calculated. A detailed description of the strontium isotope ratio and mass fraction analyses is given in the Additional file 1: Materials and methods.

Results and discussion

Petrographic characteristics of the high-fired gypsum mortars

In view of the distinguishing fine-grained debris of foraminifers, the Beautiful Pietà in the Cathedral Maria Himmelfahrt in Bozen turned out to be made of Breitenbrunn calcareous sandstone (Leitha Mountains, Burgenland, Austria) (see Additional file 2: Fig. S2, which can be found in the Results and Discussion like all Figs. Sx and Tables Sx (with x denoting numbers) mentioned below). As this finding immediately conflicts with the presumed materiality and the hypothesised South Tyrolean origin at once, the sample is not further considered in the geochemical analysis.

A minor component of the high-fired gypsum mortar of the Pietà in the Church of Our Lady of the Benedictine Abbey Marienberg is thermally stressed primary anhydrite from the gypsum deposit (approximately 5% [51, 52]) (Fig. 2). Natural carbonate impurities mainly consist of dolomite (dedolomite? [53]), partly converted after thermal decomposition and hydration to lime-lump-like grains and aggregates comprising calcite, high magnesian calcite $(Ca,Mg)CO_3$ and hydrated magnesium sulphate phases such as hexahydrite $MgSO_4 \cdot 6H_2O$ and epsomite $MgSO_4 \cdot 7H_2O$ [54] (Fig. 3). The significant presence of accompanying dolomite thus serves as criterion for narrowing down the geographic position of the exploited evaporitic sediments. Other accessory minerals scattered in the binder matrix are celestine, quartz and potassium feldspar $KAlSi_3O_8$. We interpret single marly fragments (Fig. 4) as natural impurities associated with the sulphate body and not as deliberately added ceramic aggregates.

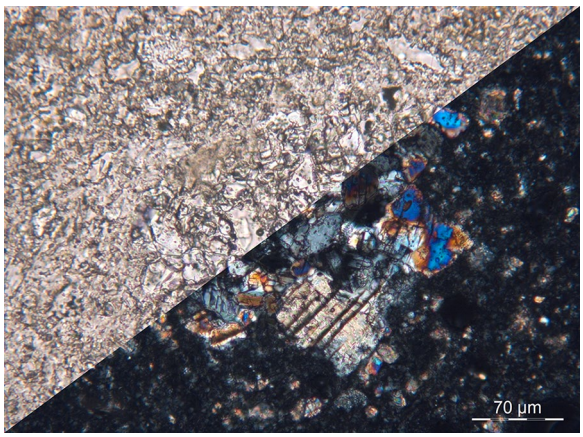

Fig. 2 Fragment of primary anhydrite with signs of thermal outgassing in the high-fired gypsum mortar constituting the Pietà in the Abbey Church Marienberg (transmitted light, parallel/crossed Nicols). In thin sections, anhydrite is clearly distinguishable from gypsum due to its higher light refraction and birefringence, i.e. in this case grey interference colours of the gypsum matrix versus up to blue interference colours of the anhydrite grains having higher relief

The petrographic characteristics of the sample belonging to the Pietà in the Chapel St. Ann in Mölten conform to the properties of the one taken from the Pietà in the Abbey Church Marienberg (Figs. 5–6).

Noticeable feature of the mortar constituting the Pietà in the Church St. Martin in Göflan is a considerable proportion of primary anhydrite of about one fourth (Figs. 7, 8). For distinguishing such natural from thermal anhydrite and establishing the medieval calcination temperatures, a recently developed Raman-spectroscopic method was applied. The crystallinity of thermal anhydrite—characterised by crystallite sizes, specific surface areas and number of crystal lattice defects—was found to rise with increasing firing temperature. This parameter can be quantified by means of the band width or full width at half maximum (FWHM), respectively, of the most prominent Raman band of anhydrite. In the present case of the cluster of fibrous anhydrite shown in Fig. 7b, a mean FWHM of 3.8 cm^{-1} (uncorrected value according to Ref. [52]) speaks for thermal anhydrite formed at around 700 °C, while the significantly higher crystallinity—and thus lower band width of approx. 3.5 cm^{-1}—of the anhydrite grains in Fig. 7c points out their primary origin. (Refs. [51, 52, 54] explain the determination of burning temperatures in the range of 600 °C to 900 °C and detail the applied peak fitting strategies for measuring FWHMs.) Beside the first-mentioned grains of firing

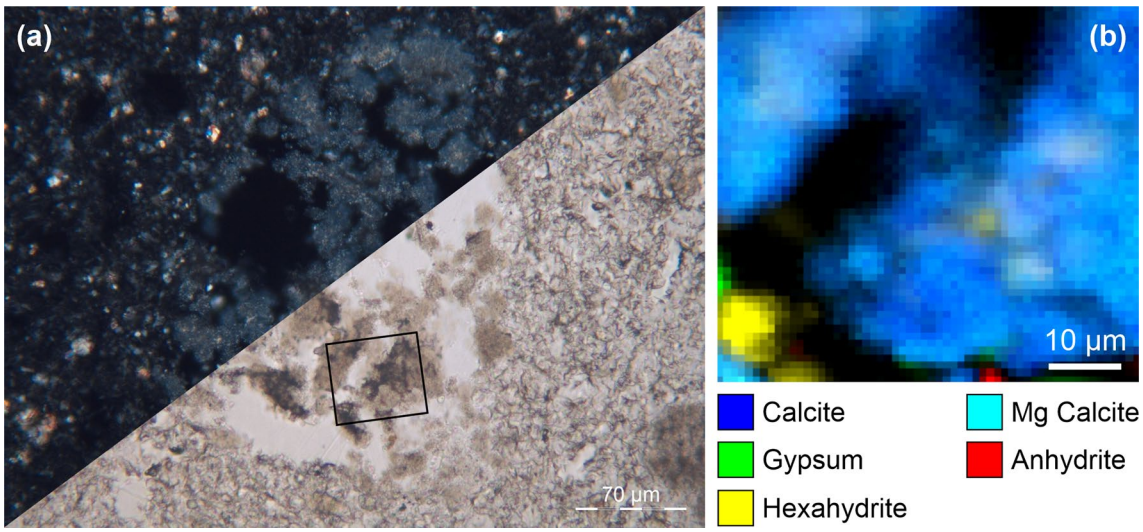

Fig. 3 Aggregate of pyrometamorphic and hydration reaction products comprising calcite, high magnesian calcite, hydrated magnesium sulphate phases (hexahydrite), anhydrite and gypsum in the binder matrix of the sample originating from the Pietà in the Abbey Church Marienberg: **a** transmitted light, crossed/parallel Nicols, and **b** Raman microspectroscopic map of the area highlighted in Fig. **a** showing phase distributions in false colours based on the intensities of marker bands. White areas are due to co-localisation along the optical axis of (high magnesian) calcite and hexahydrite

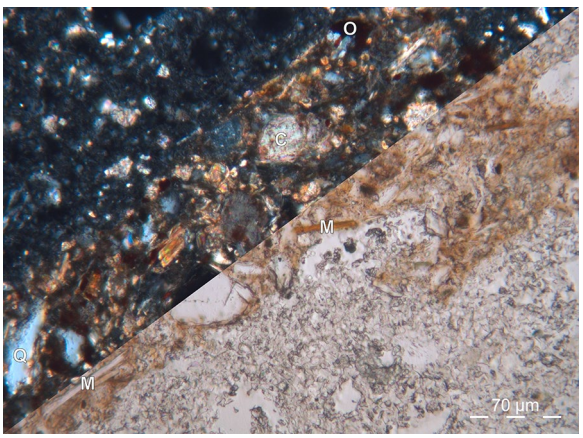

Fig. 4 Marly nodule with quartz grains (Q), carbonates (C), light and dark mica (M) and iron oxides (O) in the gypsum mortar of the Pietà in the Abbey Church Marienberg (transmitted light, crossed/parallel Nicols)

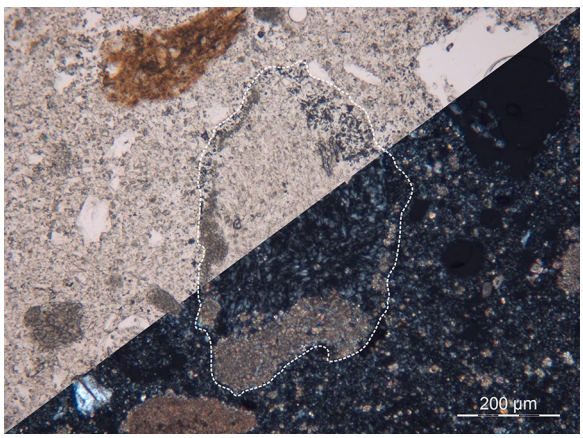

Fig. 5 In the centre a hydrated grain of firing products with carbonatic impurities—exhibiting bright, pastel interference colours due to the extremely high birefringence of calcite and dolomite—in the mortar sample belonging to the Pietà in the Chapel St. Ann in Mölten (transmitted light, parallel/crossed Nicols)

products, lime-lump-like aggregates, but also thermally undamaged calcite and rare dolomite (Additional file 2: Fig. S1) from colder temperature zones in the comminuted gypsum stones and/or the kiln are embedded in the matrix. Red to brownish mudstone and subordinate iron oxides, probably partly due to the oxidation of pyrite FeS_2 to haematite Fe_2O_3 during calcination, again trace back as natural impurities to the raw gypsum. (See Additional file 2: Table S1 for an overview of the mineralogical compositions of the materials forming the Beautiful Pietàs.)

Isotopic signature as indication of provenance

Gypsum is deposited as evaporite salt in a brine pan (sound or saline lake) after the precipitation of the alkaline earth carbonates [38, 55]. Most of the recoverable sedimentary sulphates in South Tyrol were laid down

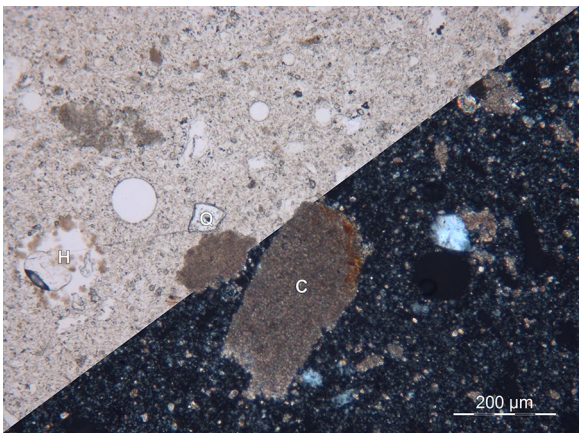

Fig. 6 Fragments of carbonatic impurities (C), an aggregate of (high magnesian) calcite and hexahydrite (H) as well as quartz grains (Q), occasionally with mineral inclusions, embedded in the binder matrix of the sample from the Pietà in the Chapel St. Ann in Mölten (transmitted light, parallel/crossed Nicols)

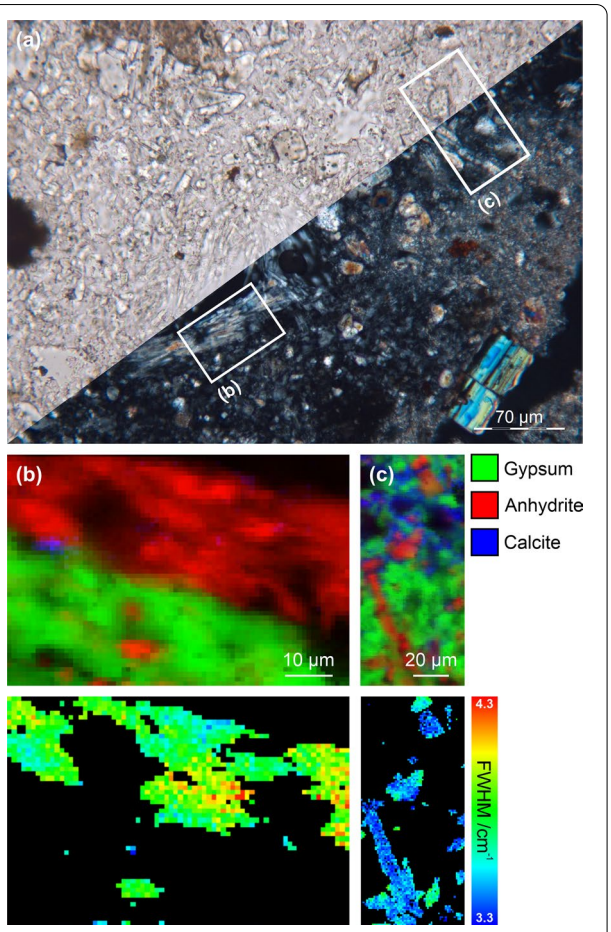

Fig. 7 Mortar sample taken from the Pietà in the Church St. Martin in Göflan: **a** transmitted light (parallel/crossed Nicols), and Raman microspectroscopic maps of **b** a cluster of fibrous thermal anhydrite crystals and **c** grains of thermally stressed primary anhydrite. FWHM denotes the full width at half maximum of the most prominent Raman band of anhydrite II, which enables to differentiate natural from thermal anhydrite and to deduce calcination temperatures, as described in the text and Ref. [52]

under the arid conditions of the Triassic period (252–201 million years ago): Marginal marine gypsum deposits of the Carnian (Upper Triassic, 237–201 Mya) are part of the Raibl Formation of the Ortler region in the Stilfs-Trafoi area (Prader alp, Patleigraben) and in the Martell Valley on the slopes of the ridge between the Madritsch and the Peder Valley ("Auf den Vertainen"). Apart from that, local gypsum concretions are to be found in the form of centimetre thick layers or maximum fist sized nodules in the Groeden Sandstone (Upper Permian, 259–251 Mya), the Bellerophon Formation (Upper Permian) and the Werfen Formation (Lower Triassic, 251–247 Mya) of the Etsch Valley (Tschöggelberg, Mendel ridge) and the Dolomites [56, 57]. In contrast to the South Tyrolean gypsum resources, the Upper Permian and Lower/Middle Triassic (Scythian/Anisian) evaporitic successions in Austria, from Hall in Tyrol in the Northern Calcareous Alps across the Salzkammergut in the broader sense and the Eastern Calcareous Alps to the gates of Vienna, were and are of great economic importance. The bodies of gypsum rocks of the Montafon and the Außerfern occur within the Raibl strata, and thus are classified as higher Carnian deposits [58–61].

Sulphates of oceanic origin of the same age show a usually very constant ratio of sulphur and strontium isotopes irrespective of the palaeographic position; fluctuations through geological time enable age determination and stratigraphic location of such evaporitic sediments. Primary gypsum, thus not affected by diagenetic reworking or post-depositional alterations (groundwater-induced recycling of sulphate ions, recrystallisation in the presence of radiogenic ^{87}Sr-bearing fluids, etc.), carries and retains the isotopic composition of the mother fluid from which it precipitated; sabkha milieu (marginal coastal salt flats) and fresh water inflow cause a shift of the values [38, 58, 62–68]. The so-far uninvestigated issue of the sensitivity of original $\delta^{34}S$ value and $^{87}Sr/^{86}Sr$ ratio to the dehydration of gypsum to anhydrite during calcination at about 900 °C, as well as to "meteoric" inflow in the form of mixing (hydration) water added to the powdered high-fired gypsum, was pursued via a small-scale burning experiment in a laboratory furnace (2 g powdered sample, 900 °C, 4 h) followed by the rehydration of the resulting binder. According to Richard Worden et al. [69] the original marine stratigraphic sulphur

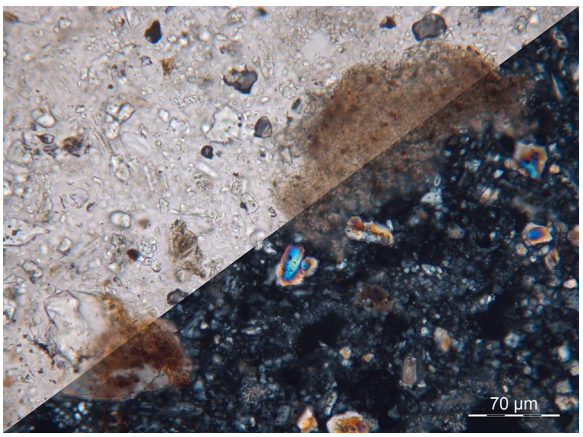

Fig. 8 Traces of the raw material embodied in the form of clayey impurities and natural anhydrite in the high-fired gypsum mortar constituting the Pietà in the Church St. Martin in Göflan (transmitted light, parallel/crossed Nicols)

isotope variation is preserved despite subsequent gypsum dehydration to anhydrite during burial alteration. It became evident, that neither the calcination of gypsum, albeit occurring in an eminently higher temperature range, involves significant isotopic fractionation. Similarly, the application of the calcium sulphate-based binder does not imply interference or masking of the primary signature in consequence of $^{87}Sr/^{86}Sr$ ratio and $\delta^{34}S$ value of the mixing water. The direct relation to the seawater remains intact not least because of the presence of accessory celestine originating from the gypsum deposit and therewith a concentration of strontium higher by several orders of magnitude compared to the mixing water; the same applies for the isotopic composition of the sulphate sulphur. Beyond that, dissolution and crystallisation reactions associated with the setting of the gypsum paste are—in contrast to large-scale geological processes, when sulphate evaporite bodies become affected by meteoric water—a single event of limited duration (no leaching, dissolution metamorphosis or repeated mineralisation processes, etc). We consider isotopic exchange reactions due to environmental influences or anthropogenic pollution of the air with sulphur components to be negligible, as the medieval figure groups were not exposed to weathering in the course of their history.

Within the framework of this study, the geographical localisation of possibly exploited deposits is pursued via the geochemical comparison of the high-fired gypsum mortars constituting the Beautiful Pietàs and reference samples of sulphate layers in South Tyrol and Austria, complemented by accessible literature data [60, 70–78]. Altogether, 78 datasets from 46 gypsum occurrences in

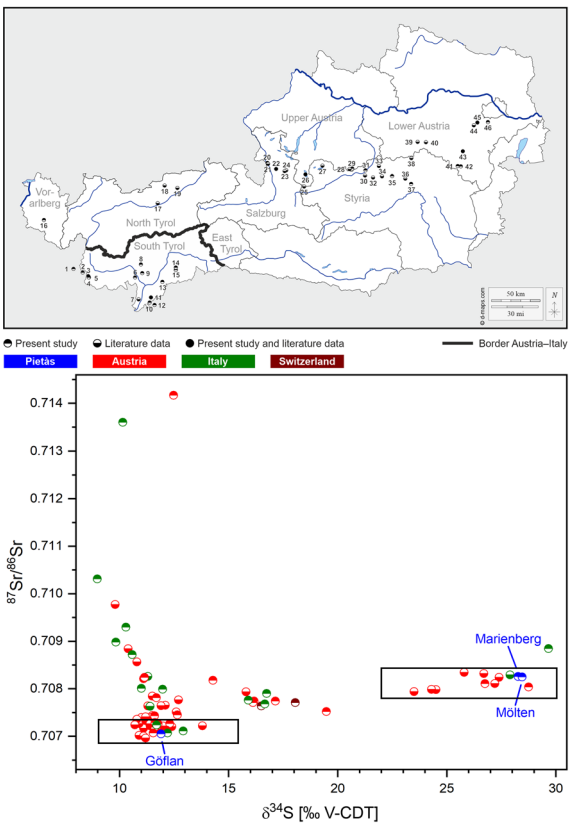

Fig. 9 Geographical distribution of evaporitic sediments (top), whose $^{87}Sr/^{86}Sr$ and $\delta^{34}S$ isotopic signatures are known from either literature or measurements undertaken within the present study. The rectangles in the graphical representation (bottom) of the isotope values of both, Beautiful Pietàs under study and gypsum stones, represent the excerpts shown in Figs. 10 and 11. The full list of locations, assigned numbers and literature references is given in Table 1

Austria, Italy and Switzerland were evaluated (Fig. 9, Table 1, Additional file 2: Fig. S3) with the aim to identify resources, which can be ruled out almost with certainty. Therefore, upper limits of uncertainty ranges around mean isotope values were estimated. Due to the intrinsic heterogeneity of the analysed materials, the calculated measurement uncertainties ($\pm 0.3‰$ for $\delta^{34}S$ and ± 0.000024 for $^{87}Sr/^{86}Sr$, both representing upper limits; in the latter case the median of all uncertainties of measurement mainly excludes exceptionally low, outlying uncertainty values) do not fully describe the inherent variations, which might be significant for the comparison of the isotope signatures; nevertheless, they were used as a starting point for the following estimations: As the mixing of calcined gypsum with water involves the homogenisation of the binder material, we estimate the characteristic standard deviations of the isotope ratios to

Table 1 Geochemical data of gypsum stones

Locality	No.	Source	$\delta^{34}S$ [‰]	$^{87}Sr/^{86}Sr$	Measurement uncertainty
Ofenpass (GR, CH)	1	Present study	+ 17.34	0.707708	0.000024
St. Maria, Val Schais (GR, CH)	2	Present study	+ 16.49	0.707637	0.000060
Furkelhütte (BZ, IT)	3	Present study	+ 16.66	0.707676	0.000024
Patleigraben (BZ, IT)	4	Present study	+ 16.74	0.707895	0.000024
Außertrafoi (BZ, IT)	5	Present study	+ 16.23	0.707765	0.000024
Prissian (BZ, IT)	6	Present study	+ 29.65	0.708846	0.000024
Tramin (BZ, IT)	7	TRAMIN 2 from Ref. [70]	+ 27.90	0.708289	0.000014
Naifjoch (BZ, IT)	8	Present study	+ 10.15	0.713604	0.000024
Mölten (BZ, IT)	9	Present study	+ 8.99	0.710330	0.000060
San Lugano/Truden (BZ, IT)	10a	Present study	+ 11.00	0.708007	0.000024
	10b	Present study	+ 10.58	0.708720	0.000024
Bletterbachschlucht (BZ, IT)	11a	Present study	+ 9.83	0.708984	0.000024
	11b	Present study	+ 11.98	0.707990	0.000024
	11c	BA 1 from Ref. [70]	+ 11.40	0.707634	0.000007
	11d	BA 5 from Ref. [70]	+ 11.30	0.708262	0.000007
Cavalese (TN, IT)	12	Present study	+ 11.70	0.707242	0.000024
Schlern (BZ, IT)	13	Present study	+ 9.58	0.709298	0.000024
Weißlahn/Aferer Geißler (BZ, IT)	14	Present study	+ 12.21	0.707070	0.000024
Tschantschenon (BZ, IT)	15	Present study	+ 12.92	0.707109	0.000024
St. Anton im Montafon (V, AT)	16	Present study	+ 17.14	0.707742	0.000024
Hall in Tirol (T, AT)	17	KÖ 4 from Ref. [70]	+ 24.50	0.707984	0.000009
Sulzgraben, Plumsjoch (T, AT)	18	SU 2 from Ref. [70]	+ 12.70	0.707764	0.000008
Schichthals, Rofangebirge (T, AT)	19	SCHI 3 from Ref. [70]	+ 15.80	0.707935	0.000009
Hallein (S, AT)	20	Present study	+ 19.48	0.707520	0.000024
Dürrnberg, Hallein (S, AT)	21a	SCHL 5 from Ref. [70]	+ 11.10	0.707169	0.000009
	21b	SCHE 4 from Ref. [70]	+ 10.90	0.707285	0.000009
	21c	O 13/9 from Ref. [70]	+ 10.80	0.708563	0.000013
	21d	A 5 from Ref. [70]	+ 11.50	0.707843	0.000012
Grubach-Moosegg (S, AT)	22a	Present study	+ 12.65	0.707455	0.000024
	22b	Present study	+ 11.62	0.707187	0.000024
	22c	MO 14 from Ref. [70]	+ 13.80	0.707220	0.000008
	22d	MO 26 from Ref. [70]	+ 12.40	0.707197	0.000007
	22e	Present study	+ 11.55	0.707067	0.000024
Webing (S, AT)	23	WE 23 from Ref. [70]	+ 12.10	0.707651	0.000019
Grub (S, AT)	24	GRUB 4 from Ref. [70]	+ 10.90	0.707017	0.000012
Karlgraben, Ramsau (ST, AT)	25	K 3 from Ref. [70]	+ 11.00	0.707394	0.000009
Hallstatt (UA, AT)	26a	Present study	+ 14.13	0.708179	0.000024
	26b	Present study	+ 28.96	0.708039	0.000024
	26c	FJ 17 from Ref. [70]	+ 27.40	0.700824	0.000026
	26d	E 6 from Ref. [70]	+ 10.90	0.707269	0.000008
	26e	TS 26 from Ref. [70]	+ 9.80	0.709773	0.000011
	26f	TS 37 from Ref. [70]	+ 10.40	0.708839	0.000020
	26 g	A 12 from Ref. [70]	+ 11.90	0.707643	0.000012
Wienern, Grundlsee (ST, AT)	27a	WB 20 from Ref. [70]	+ 24.30	0.707986	0.000025
	27b	WA 1G from Ref. [70]	+ 12.00	0.707216	0.000008
	27c	WD 1 from Ref. [70]	+ 12.60	0.707511	0.000019
Hintersteiner Alm, Pyhrnpass (UA, AT)	28a	HIN 4 from Ref. [70]	+ 11.20	0.707329	0.000011
	28b	HIN 12 from Ref. [70]	+ 10.80	0.707354	0.000015
Fuchsalm, Spital am Pyhrn (UA, AT)	29	Present study	+ 11.61	0.707431	0.000024

Table 1 (continued)

Locality	No.	Source	$\delta^{34}S$ [‰]	$^{87}Sr/^{86}Sr$	Measurement uncertainty
Schildmauer, Admont (ST, AT)	30a	SLD 5 from Ref. [70]	+ 25.80	0.708345	0.000011
	30b	SLD 15 from Ref. [70]	+ 26.70	0.708317	0.000011
Weng, Admont (ST, AT)	31	Present study	+ 11.77	0.707263	0.000024
Johnsbachtal (ST, AT)	32	WO 2 from Ref. [70]	+ 11.60	0.707310	0.000013
Kaswassergraben (ST, AT)	33a	KWGR from Ref. [70]	+ 27.20	0.708107	0.000016
	33b	KWG 6from Ref. [70]	+ 11.10	0.707004	0.000019
Schießengraben, Radmer (ST, AT)	34	RAD 6 from Ref. [70]	+ 11.10	0.708210	0.000039
Eisenerz (ST, AT)	35	Present study	+ 12.48	0.714167	0.000024
Tragöß-Oberort (ST, AT)	36a	TR 6 from Ref. [70]	+ 11.40	0.707222	0.000011
	36b	TR 17 from Ref. [70]	+ 11.20	0.706963	0.000025
Lamingtal, Bruck an der Mur (ST, AT)	37a	Present study	+ 11.15	0.708240	0.000024
	37b	Present study	+ 11.63	0.707292	0.000024
	37c	Present study	+ 11.52	0.707269	0.000024
Dürradmer, Mariazell (ST, AT)	38	DÜ 2 from Ref. [70]	+ 11.70	0.707164	0.000011
Trübenbach, Ötscher (LA, AT)	39	TB 1 from Ref. [70]	+ 23.50	0.707939	0.000017
Annaberg (LA, AT)	40	BERG 3 from Ref. [70]	+ 11.40	0.707262	0.000035
Haidbachgraben, Semmering (LA, AT)	41	Present study	+ 16.17	0.707739	0.000024
Göstritz (LA, AT)	42	Present study	+ 16.12	0.707712	0.000024
Pfennigbach, Puchberg am Schneeberg (LA, AT)	43a	Present study	+ 12.15	0.707125	0.000024
	43b	PF 1 from Ref. [70]	+ 11.50	0.707437	0.000024
	43c	PF 5 from Ref. [70]	+ 11.50	0.707410	0.000018
Alland-Groisbach (LA, AT)	44	AHGI from Ref. [70]	+ 10.70	0.707241	0.000024
Preinsfeld, Heiligenkreuz (LA, AT)	45a	Present study	+ 11.69	0.707809	0.000024
	45b	PR 3 from Ref. [70]	+ 11.20	0.707407	0.000011
	45c	PR 1 from Ref. [70]	+ 11.30	0.707637	0.000021
Mödling (LA, AT)	46	Present study	+ 26.76	0.708107	0.000024

IT Italian, *BZ* provinces of Bozen/South Tyrol, *TN* Trento, *CH* Swiss, *GR* canton of the Grisons, *AT* Austrian, *V* Länder of Vorarlberg, *T* Tyrol, *S* Salzburg, *ST* Styria, *UA* Upper Austria, *LA* Lower Austria

be equal to their measurement uncertainties. This does not hold true for the reference materials taken from sulphate bodies of different heterogeneity and thickness, as the exact sampling location within a deposit or quarry might substantially affect the geochemical results. In fact, resampling of gypsum stones led—in contrast to repeated isotope analyses of the medieval mortars—to isotope values matching only within twice their measurement uncertainties. Hence, here we estimate the—a priori unknown—standard deviations to equal ± 0.6‰ for $\delta^{34}S$ and ± 0.000048 for $^{87}Sr/^{86}Sr$.

In case of normally distributed measurement values, a mean ± its double standard deviation theoretically covers 95.5% of the data. We therefore defined a missing overlap between twice the assumed standard deviations of gypsum mortar ($2\sigma = 0.6$‰ for $\delta^{34}S$ and 0.000048 for $^{87}Sr/^{86}Sr$, respectively) and reference sample ($2\sigma = 1.2$‰ for $\delta^{34}S$ and 0.000096 for $^{87}Sr/^{86}Sr$, respectively) as the criterion for excluding potential raw materials with high probability. Gypsum stones overlapping in both their sulphur and strontium isotopic signature can be graphically identified by plotting mean values as the centres of rectangles in $^{87}Sr/^{86}Sr$ versus $\delta^{34}S$ diagrams, whose dimensions represent the 2σ criterion (see Figs. 10, 11). In the following, the 14 evaporitic sediments (represented by 15 datasets) among the 46 considered Austroalpine gypsum deposits (78 datasets) fulfilling this condition, are further reflected upon their composition in terms of secondary constituents and subordinate minerals. Being aware that the standard deviation is—even though based on calculated measurement uncertainties—only an estimation, we would like to point out that even doubling of the sulphur isotope ranges would not change the presented outcome insofar, as only some other samples from the most plausible occurrences would emerge as additional candidates.

The isotopic signature of the gypsum mortar of the Pietà in the Church St. Martin in Göflan ($\delta^{34}S + 11.9$‰, $^{87}Sr/^{86}Sr$ 0.707052) matches Upper Permian evaporites [62, 65]. It correlates with the one of the South Tyrolean

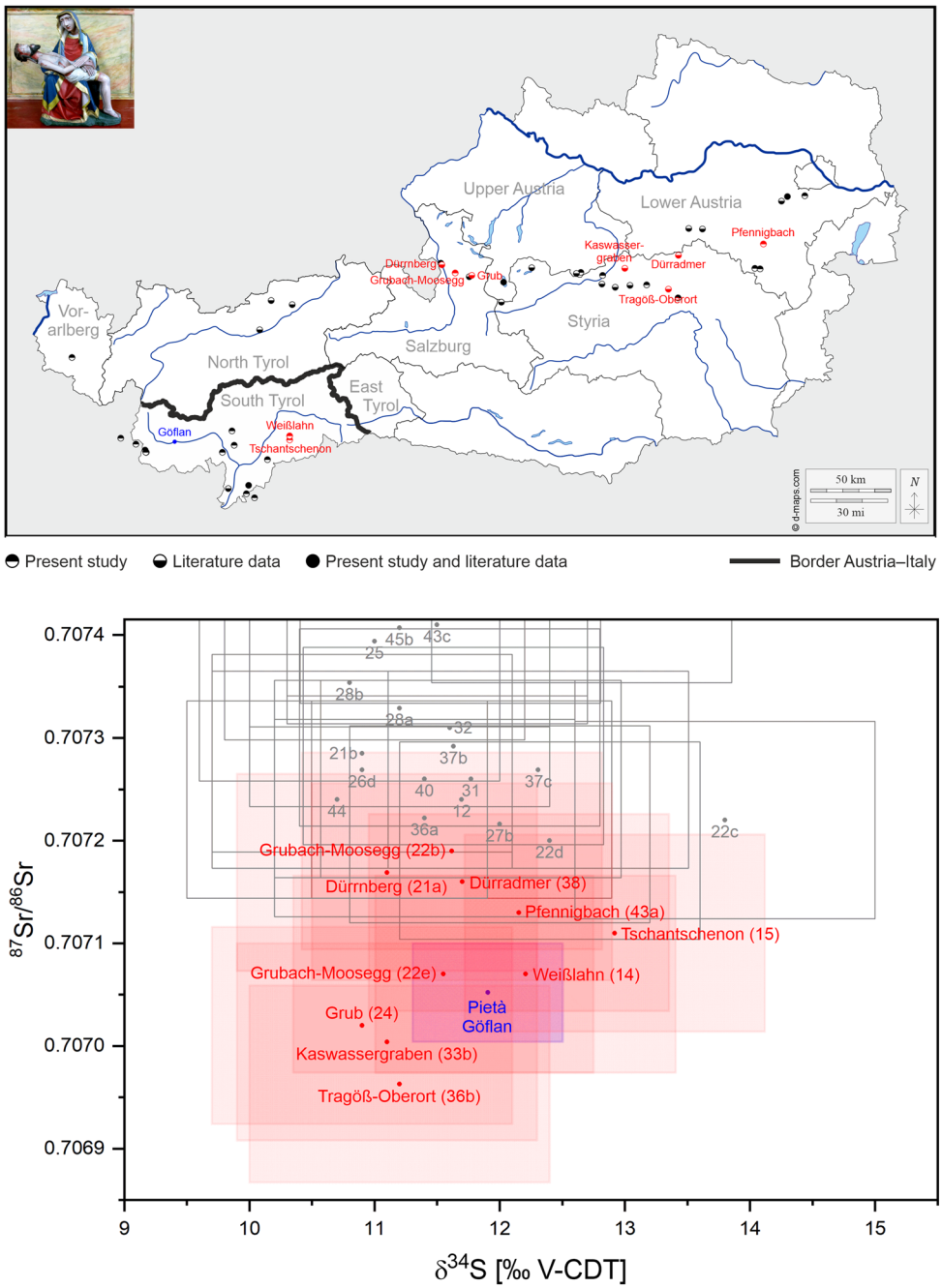

Fig. 10 Geographical locations (top) and $^{87}Sr/^{86}Sr$ versus $\delta^{34}S$ diagram (bottom) of gypsum bodies, which according to the 2σ criterion defined in the text match (red rectangles in the bottom diagram) with the geochemical signature of the mortar constituting the Pietà in the Church St. Martin in Göflan (blue)

reference samples Tschantschenon and Weißlahn/Aferer Geißler in the Villnöss Valley (Fig. 10), which, however, can be excluded as raw material in view of their very small percentage of anhydrite and their significant amount of dolomite (Additional file 2: Table S2). Furthermore, the resulting values are in accordance with anhydrite and alabaster gypsum of Grubach-Moosegg near Golling (Salzburg) as well as gypsum originating from the quarry Pfennigbach near Puchberg am Schneeberg (Lower Austria). Eberhard Fugger describes the

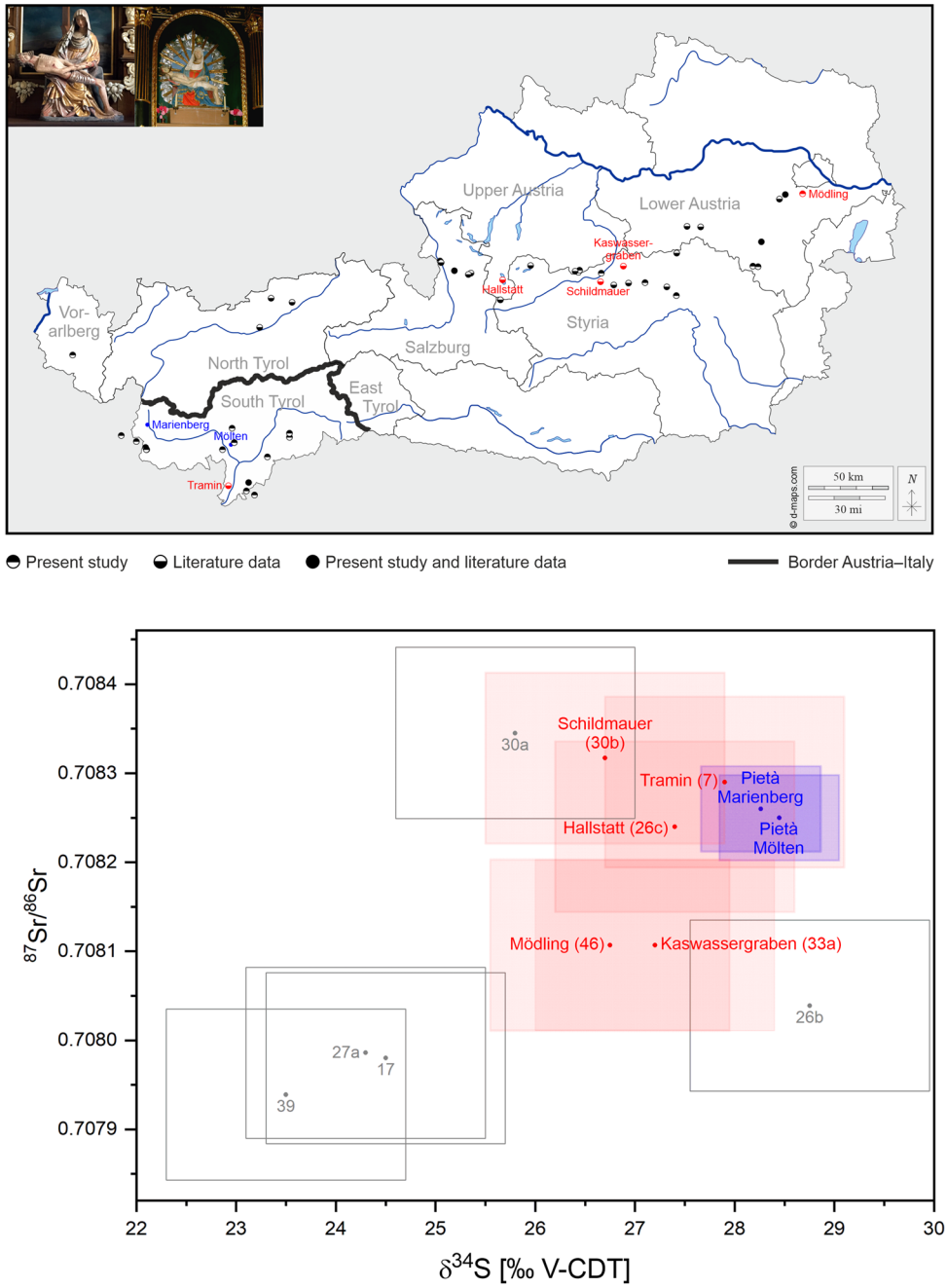

Fig. 11 Geographical locations (top) and comparison of isotope signatures (bottom) of the high-fired gypsum mortars sampled from the Pietà in the Abbey Church Marienberg and the Pietà in the Chapel St. Ann in Mölten (blue) with the $^{87}Sr/^{86}Sr$ and $\delta^{34}S$ values of deposits (red), which might have been exploited for binder production

deposit of Grubach-Moosegg in 1878 as the presumable largest one in the Alps exposed without overlaying cap rock [79, 80]. The dominant sulphate bodies, hosting sulphide mineralisation including rare lead sulphosalts, are tectonically mixed with subordinate lenses of dark dolomite, dark-grey, green and red mudstones, pelagic limestones and marls, abundant plutonic and volcanic as well as rare metamorphic (serpentinite) rocks [58, 81–85]. In both of the samples, the minerals calcite, magnesite, potassium feldspar, celestine and pyrite are detectable by means of microspectroscopic techniques in addition to the major components anhydrite and gypsum

(Additional file 2: Table S2, Fig. S4). The reference Pfennigbach, again containing anhydrite, calcite, magnesite, dolomite, celestine, potassium feldspar and pyrite as geologically related accessories (Additional file 2: Table S2, Figs. S6–S8 and Ref. [86]), also pertains to one of the most extensive gypsum resources in the Eastern Alps, intercalated in argillaceous slate and slaty sandstones of the Werfen strata.

According to the geochemical data sets published by Christoph Spötl and Edwin Pak in 1996 [70] the deposits Grub near Abtenau and Dürrnberg above Hallein (Salzburg) in the Salzkammergut and Kaswassergraben in the Tamischbach Valley near Großreifling, Tragöß-Oberort and Dürradmer near Mariazell (Styria) in the Eastern Calcareous Alps come into question as raw material as well. Here again the minor and trace compounds mentioned in the literature do not allow to deduce concrete approaches for a shortlist, as similar and besides that consistent with the mineralogical properties of the high-fired gypsum mortar sampled from the Pietà in the Church St. Martin in Göflan:

The abandoned quarry Grub, depicted by Eberhard Fugger in 1878 as a gypsum body with marly and clayey impurities [79], lies associated with carbonates, haematite and copper iron sulphides plus vulcanite fragments in Werfen slates [83]. The presence of a mélange of anhydrite nodules and beds, rock salt, saliferous clay and gypsum in facies of the Haselgebirge Formation of the salt mine Dürrnberg is already mentioned by Eberhard Fugger, too, [79] and confirmed by Christoph Spötl in 1988 with complementary remarks on traces of a copper mineralisation [74]. The gorge Kaswassergraben exposes pervasively deformed Haselgebirge evaporites, fine-grained siliciclastic and carbonate rocks [70, 87, 88]. The essential characteristic of subordinate magnesite is not in line with the medieval gypsum mortar of relevance here. However, the hitherto absence of evidence of magnesite might be due to thermal decomposition to periclase MgO at about 680 °C to 700 °C [89, 90] as well as slow hydration and carbonation via intermediate steps [91–94]. Gypsum layers interbedded with Werfen slates, quartzite, dark grey limestones and calciferous slates typify the gypsum mine Tragöß-Oberort. Also the deposit Dürradmer is associated with Werfen strata; a red and green argillaceous slate and sandstone horizon separates an alternation of gypsum, dolomite and anhydrite from nearly pure gypsum [95, 96].

The isotopic fingerprints of the high-fired gypsum mortars forming the two Pietàs in the Church of Our Lady of the Benedictine Abbey Marienberg ($\delta^{34}S + 28.3‰$, $^{87}Sr/^{86}Sr$ 0.708262) and in the Chapel St. Ann in Mölten ($\delta^{34}S + 28.4‰$, $^{87}Sr/^{86}Sr$ 0.708255) are consistent within the measurement uncertainty and diagnostic of Early Triassic evaporites or successions of the Lower-Middle Triassic transition [62, 65], which points to gypsum deposits in the Werfen or Reichenhall Formation as raw material. Among the own Eastern Alpine reference samples only gypsum from Mödling (Lower Austria) in the southern conurbation of Vienna shows values of the Scythian/Anisian boundary (Fig. 11), including a matching mineralogical composition (Additional file 2: Table S2). From an art historical perspective this coherence is intriguing insofar, as the identification of the material of the Pietà in the cathedral Maria Himmelfahrt in Bozen as Breitenbrunn calcareous sandstone necessitates to establish ties to a workshop operating in the Vienna area. Moreover, distinct details such as Mary's tightly belted dress, the drapery of the veil or the fringe blanket of the throne bench seem to be unique features of these three figure groups plus the Beautiful Pietà in the Church St. Andrew in Lienz (East Tyrol) [97].

To be considered isotope data from the literature [70, 77, 98, 99] concern sediments close to Tramin in the South Tyrolean Etsch Valley and the salt mountain Hallstatt in the Upper Austrian Salzkammergut. The gypsum lenses Kaswassergraben near Großreifling and Schildmauer near Admont, both in Styria, only narrowly meet the specified selection criterion of the double standard deviation. Concretionary nodules and centimetre thick layers occurring within silty marlstones and limestones of the Lower Triassic Werfen Formation (Cencenighe Member) in the gorge Höllental and the Lungenfrischgraben in the vicinity of Tramin can be ruled out, as predominantly accompanied by carbonate minerals in the form of calcite [77]. In turn, the deposit of bituminous dolomitic/anhydritic grey salt rock in the salt mine of Hallstatt is described in mineralogical consistency with the sampled medieval mortars as monotone alternation of calcite/dolomite (partially dedolomitised) and anhydrite beds [59, 70, 74] (see also Additional file 2: Fig. S5). As already mentioned, the processing of gypsum originating from the Kaswassergraben should result in the presence of magnesite or its decomposition, hydration and carbonation products in the binder matrix of the high-fired gypsum mortars of both of the Beautiful Pietàs, but evidence is lacking at least based on the available sample material. According to Johann Haditsch and Otto Ampferer, copper mineralisation (devilline $CaCu_4(SO_4)_2(OH)_6{\cdot}3H_2O$, chalcopyrite $CuFeS_2$), fahlore (comprising bornite Cu_5FeS_4 and galena PbS), pyrite and haematite are to be found in the dolomite rich gypsum and anhydrite deposit Schildmauer, a detached sedimentary layer wrapped in Werfen slates [87, 100]. Christoph Spötl and Edwin Pak characterise the dark grey dolomite beds alternating with gypsum as peloidal packstones, partly containing accessory detrital quartz [70] – a classification not met by the

dolomitic or rather carbonatic components of the mortars constituting the figure groups in the Abbey Church Marienberg and the Chapel St. Ann in Mölten.

Conclusions and outlook

The combination of petrography (secondary constituents and subordinate minerals) and geochemistry ($\delta^{34}S$ value and $^{87}Sr/^{86}Sr$ ratio) allows to overcome the absence of medieval documentary sources by establishing a connection between Austroalpine raw materials and high-fired gypsum mortars constituting three of the examined Gothic figure groups: the Upper Permian and Early Triassic sulphate deposits exploited for the creation of the Pietà in the Church St. Martin in Göflan as well as the two metrologically consistent sculptures in the Church of Our Lady of the Benedictine Abbey Marienberg and the Chapel St. Ann in Mölten are probably not located in South Tyrol, but in the Salzkammergut in the Haselgebirge Formation at the base of the Austrian Northern Calcareous Alps or in the Eastern Calcareous Alps. Thus, the results back up the hypothesis of an import of the figure groups shaped around 1400 in specialised workshops in the archdiocese of Salzburg and the duchies of Austria and Styria or rather the present Austrian Länder Salzburg, Upper and Lower Austria or Styria. (In contrast, the isotopic signatures of Early Medieval stucco fragments of St. Peter above Gratsch correlate with the fingerprint of Carnian gypsum layers in the Upper Vinschgau, which, in turn, cannot be differentiated from outcrops of the same age in the Schais Valley in the neighbouring Swiss canton of Grisons [101]).

It would be desirable to add distinct historical and archival threads of information on medieval mining to the geochemical discussion. The oldest reference to the application of gypsum as building or artist material in Austria dates back to the year 1465 (entry in the account book of the Benedictine Abbey Nonnberg in Salzburg), however without any indication of origin [102]. According to the mining area and dump register of the Geologische Bundesanstalt, gypsum is mined in the Salzkammergut at Grubach-Moosegg at least since 1613 [85], at Grub between 1963 and 1978; corresponding data concerning the exploitation of the deposits Dürrnberg (1185 until 1989) and Hallstatt (1311 till present) most probably only refer to the mining of rock salt. The quarry Pfennigbach in the Eastern Calcareous Alps is in operation with interruptions since around 1860, the mine Mödling from 1840 until 1912. Quarrying of the gypsum lenses Kaswassergraben and Schildmauer is documented in the nineteenth century and from 1961 until 1991, respectively, similar activities at Tragöß-Oberort since 1966, while the sulphate body Dürradmer is hitherto unexploited [103].

Taking up the current art historical problem in regard to the provenance of the ensemble of Beautiful Pietàs, still venerated today in South Tyrol in small village churches and chapels, with natural scientific methods, the present study yields novel insights of not only local relevance, but disposes the basis for further analyses extendable to a supra-regional level, as quite numerous figure groups of this type have been preserved in Central Europe and the Apennines. The contradictory information regarding their materiality and the sparse published analytical results concerning exemplars made of high-fired gypsum mortar [104–111] allow the broadening of the research question to encompass materials sciences and art technology. If future petrographic and geochemical studies reveal further clustering, this may spark art historical research.

Supplementary Information

The online version contains supplementary material available at https://doi.org/10.1186/s40494-022-00678-6.

Additional file 1. Materials and methods.

Additional file 2. Results and discussion.

Acknowledgements

We gratefully acknowledge Werner Kuntner (St. Martin, Göflan), dean Bernhard Holzer (Cathedral of Bozen), abbot Bruno Trauner (Abbey Marienberg) as well as Angelika Wiedmer and Alfons Stanger (Chapel St. Ann, Mölten) for consenting to the sampling of the Beautiful Pietàs. We furthermore thank Uwe Kolitsch (Natural History Museum, Vienna, Austria), Albert Schedl (Geologische Bundesanstalt, Vienna, Austria) and Ralf-Thomas Schmitt (Museum für Naturkunde, Berlin, Germany) for providing reference samples of Austroalpine gypsum deposits.

We would like to thank Martin Rosner for helpful advice and Maren Koenig for conducting the sample preparation for strontium isotope analyses at the Federal Institute for Materials Research and Testing (BAM), Berlin.

The Raman spectra shown in Additional file 2: Figs. S4–S8 in the Results and Discussion were acquired by Alina Zettner within the frame of a student internship at BAM, Berlin, supervised by TS.

We highly value the accurate linguistic comments of Stéphanie Weinberger on the manuscript.

Authors' contributions

PD had the idea for and designed the study, wrote the main body of this text, performed the polarised light microscopy analyses and interpreted the microscopic, microspectroscopic and geochemical results. UGW and JV carried out the sulphur and strontium isotope analyses, respectively, and wrote the related sections about experimental methods and evaluations; JV authored the Additional file 1: Materials and Methods. TS conducted the Raman microspectroscopic measurements, combined and statistically evaluated the sulphur and strontium isotope data, provided the according figures and text and contributed to the interpretation of the results. TS and PD composed the Additional file 2: Results and discussion. All authors read and approved the final manuscript.

Funding

Open Access funding enabled and organised by Projekt DEAL. This work was partly funded by the Foundation Heritagelab, Bozen, Italy (www.heritagelab.art).

UGW was supported by a Discovery Grant of the National Science and Engineering Research Council of Canada.

Availability of data and materials
All isotope data ($\delta^{34}S$ and $^{87}Sr/^{86}Sr$) generated or analysed during this study are included in Table 1 in this published article. Further datasets, such as Raman spectra, acquired and/or analysed during the current study are available from the corresponding author on reasonable request.

Declarations

Competing interests
The authors declare that they have no competing interests.

Author details
[1]Heritagelab, 39100 Bozen, Italy. [2]Department of Earth Sciences, University of Toronto, Toronto M5S 3B1, Canada. [3]Department of Analytical Chemistry, Reference Materials, Federal Institute for Materials Research and Testing, 12489 Berlin, Germany.

Received: 10 January 2022 Accepted: 9 March 2022
Published online: 25 March 2022

References

1. Pinder W. Zum Problem der„Schönen Madonnen" um 1400. Jahrbuch der Preußischen Kunstsammlungen. 1923;44:147–71.
2. Körte W. Deutsche Vesperbilder in Italien. Kunstgeschichtliches Jahrbuch der Bibliotheca Hertziana. 1937;1:1–138.
3. Clasen K. Die Schöne Madonna, ihr Meister und seine Nachfolger. Königstein im Taunis: Karl Robert Langewiesche Verlag; 1957.
4. Clasen K. Der Meister der Schönen Madonnen. Herkunft, Entfaltung und Umkreis. Berlin: De Gruyter; 1974.
5. Schultes L. Die Pietà von Celje und eine Gruppe von Vesperbildern des Schönen Stils. In: Höfler J, editor. Gotik in Slowenien. Ljubljana: Narodna Galery; 1995. p. 173–81.
6. Der FA. Meister der Schönen Madonnen. Zeitschrift des deutschen Vereins für Kunstwissenschaft. 1943;10:19–48.
7. Suckale R. Review about Clasen K. Der Meister der Schönen Madonnen Herkunft. Entfaltung und Umkreis Berlin: De Gruyter. 1974;29:244–55.
8. Schwarz M. Höfische Skulptur im 14. Jahrhundert. Entwicklungsphasen und Vermittlungswege im Vorfeld des Weichen Stils. Worms: Wernersche Verlagsgesellschaft; 1986.
9. Müller C. Mittelalterliche Plastik Tirols. Berlin: Deutscher Verein für Kunstwissenschaft; 1935.
10. Kutal A. Le„belle" pietà italiane. Bollettino dell'Istituto storico cecoslovacco a Roma 1946;2:7–30.
11. Paatz W. Prolegomena zu einer Geschichte der deutschen spätgotischen Skulptur im 15 Jahrhundert. Heidelberg: C. Winter; 1956.
12. Kutal A. České gotické sochařství 1350–1450. Prague: Státní nakladatelství krásné literatury a umění; 1962.
13. Großmann D (1965) Salzburgs Anteil an den "Schönen Madonnen". In: Schöne Madonnen 1350–1450. Salzburg: Salzburger Domkapitel. 1965. p. 24–44.
14. Großmann D. Thema und Variation – Austauschbarkeit der Formen in der Kunst um 1400. In: Pochat G, Wagner B, editors. Internationale Gotik in Mitteleuropa. Graz: Akademische Druck- und Verlagsanstalt; 1991. p. 162–73.
15. Rossacher K. Zum Problem des Vesperbildes um 1400. Alte und moderne Kunst. 1970;112:2–7.
16. Neuhardt J, Schütz W. Die Pietà. Freilassing: Pannonia-Verlag; 1972.
17. Schmidt G. Vesperbilder um 1400 und der "Meister der Schönen Madonnen." Österreichische Zeitschrift für Kunst und Denkmalpflege. 1977;31:94–114.
18. Schmidt G. Review about Clasen K. Der Meister der Schönen Madonnen Herkunft, Entfaltung und Umkreis. Zeitschrift für Kunstgeschichte. 1978;41:61–92.
19. Steingräber E. Zur Italianisierung des deutschen Vesperbildes. In: Kashnitz R, Volk P, editors. Skulptur in Süddeutschland 1400–1770. Munich: Deutscher Kunstverlag; 1998. p. 11–6.
20. Castri S. *In virginis gremium repositus*. Dall'archetipo del Vesperbild alla 'Bella Pietà': un excursus, non solo alpino. In: Castelnuovo E, de Gramatica F, editors. Il gotico nelle Alpi 1350–1450. Trento: Castello del Buonconsiglio; 2002. p. 170–85.
21. Schröder J. Das Eckige muss ins Runde–das Horizontale Vesperbild als "Suche nach dem Kanon." Ars. 2004;37:40–67.
22. Söding U. Schöne Madonnen in Bayern, Schwaben und Tirol. In: Jarošová M, Kuthan J, Scholz S, editors. Prag und die großen Kulturzentren Europas in der Zeit der Luxemburger (1310–1437). Prague: Charles University; 2008. p. 183–207.
23. Kvapilová L. Vesperbilder in Bayern von 1380 bis 1480 zwischen Import und heimischer Produktion. Petersberg: Michael Imhof Verlag; 2017.
24. Weniger M. Die Schönen Vesperbilder und der Kunstexport aus Prag und Böhmen. Fragen der Methode und Zwischenbericht. In: Hrbáčová J, editor. Piety krásného slohu. Muzeum umění: Olomouc; 2017. p. 33–40.
25. Söding U. "Das Bild, welches von Prag kam". Zur Verbreitung der Schönen Madonnen und Vesperbilder. In: Březová D, Kuthan J, Peroutková J, Scholz S, editors. Kaiser Karl IV. Die böhmischen Länder und Europa. Prague: Charles University; 2017. p. 194–218.
26. Hlobil I. Salzburger Schöne Madonnen aus gegossenem Kunststein. In: Hlobil I, Mayrhofer H, Winzeler M, Chlumská Š, editors. Schöne Madonnen aus Salzburg. Gussstein um 1400. Prague: National gallery Prague; 2019. p. 38–57.
27. Großmann D. Die Breslauer "Schöne Madonna" und ihr Typus in Westdeutschland. Städel-Jahrbuch. 1977;6:231–64.
28. Castelnuovo E. Le Alpi, crocevia e punto d'incontro delle tendenze artistiche nel XV secolo. Ricerche di storia dell'arte 1978/79;9:5–12.
29. Bernini R. Vesperbilder in territorio bellunese. In: Spiazzi A, editor. A nord di Venezia. Scultura e pittura nelle vallate dolomitiche tra Gotico e Rinascimento. Milan: Silvana Editoriale; 2004. p. 299–303.
30. Springer L. Die bayrisch-österreichische Steingußplastik der Wende vom 14. zum 15. Jahrhundert. Würzburg: Werkbunddruckerei; 1936.
31. Springer L. Das Vesperbild von Meltina, ein Meisterwerk alpenländischer Bildhauerkunst des frühen 15. Jahrhunderts Der Schlern. 1937;18:80–3.
32. Rasmo N. Il Crocifisso ligneo di San Giorgio Maggiore a Venezia. In: Benesch O, editor. Festschrift für Karl Swoboda. Vienna: R.M. Rohrer; 1959. p. 237–43.
33. Kreuzer-Eccel E-M. Ein „schönes Vesperbild" im Bozner Museum. In: Grabmayr V, Mackowitz H, editors. Festschrift Otto R. v. Lutterotti. Innsbruck: Kommissionsverlag der österreichischen Kommissionsbuchhandlung; 1973. p. 273–91.
34. Kreuzer-Eccel E-M. Hans von Judenburg und die Plastik des weichen Stiles in Südtirol. Calliano: Vallagarina arti grafiche R. Manfrini AG; 1976.
35. Rasmo N. Una scultura medioevale inedita, la pietà di Cavalese. Cultura Atesina. 1948;4:125–7.
36. Rasmo N. La Pietà di Legnago. Legnago: Editrice dell'Archeoclub d'Italia; 1984.
37. Caesar C. Der "Wanderkünstler". Ein kunsthistorischer Mythos. Berlin: LIT Verlag; 2012.
38. Evaporites WJ. A geological compendium. Cham: Springer International Publishing; 2016.
39. Deer W, Howie R, Zussman J. An introduction to the rock-forming minerals. Harlow: Pearson Prentice Hall; 1992.
40. Visser H, Wolter A. Hochbrandgipsmörtel in Norddeutschland: Herkunft, Verbreitung, Bestandteile. In: Jonkanski D, Reimers H, Seidel H, editors. Kirchen aus Gips–Die Wiederentdeckung einer mittelalterlichen Bauweise in Holstein. Kiel: Verlag Ludwig; 2017. p. 72–91.
41. Lenz R, Sobott R. Beobachtungen zu Gefügen historischer Gipsmörtel. In: Auras M, Zier H-W, editors. Gipsmörtel im historischen Mauerwerk und an Fassaden. Munich: WTA Publications; 2008. p. 23–34.
42. Schlütter F, Jakubek M, Juling H. Charakterisierung und Eigenschaften historischer Gipsmörtel aus unterschiedlichen Epochen und Anwendungsgebieten. In: Institut für Steinkonservierung (IFS), editor. Gips als Baugrund, Mörtel und Dekorationsmaterial. Mainz: IFS; 2012. p. 49–59.
43. Schlütter F. Mittelalterlicher Hochbrandgips. In: Brandenburgisches Landesamt für Denkmalpflege und Archäologisches Landesmuseum, editor. 800 Jahre Kunststein – vom Imitat zum Kunstgut. Worms: Wernersche Verlagsgesellschaft mbH; 2012. p. 27–39.
44. Torres J, Mendez J, Sukiennik M. Transformation enthalpy of the alkali-earths sulfates ($SrSO_4$, $CaSO_4$, $MgSO_4$, $BaSO_4$). Thermochim Acta. 1999;334:57–66.

45. Şener S, Bilgen S, Özbayogglu G. Effect of heat treatment on grindabilities of celestite and gypsum and separation of heated mixture by differential grinding. Miner Eng. 2004;17:473–5.
46. Lafuente B, Downs R, Yang H, Stone N. The power of databases: the RRUFF project. In: Armbruster T, Danisi RM, editors. Highlights in mineralogical crystallography. Berlin: W. De Gruyter; 2015. p. 1–30.
47. Schmid T, Dariz P. Raman microspectroscopic imaging of binder remnants in historical mortars reveals processing conditions. Heritage. 2019;2:1662–83.
48. Coplen T, Hopple J, Böhlke J, Peiser H, Rieder S, Krouse H, Rosman K, Ding T, Vocke R, Révész K, Lamberty A, Taylor P, De Bièvre P. Compilation of minimum and maximum isotope ratios of selected elements in naturally occurring terrestrial materials and reagents. Water-Resources Investigations Report 01–4222. Reston: US Department of the Interior, US Geological Survey; 2002.
49. Faure G, Mensing T. Isotopes: principles and applications. Hoboken: Wiley; 2013.
50. http://georem.mpch-mainz.gwdg.de. Accessed 12 Dec 2021.
51. Dariz P, Jakob C, Ectors D, Neubauer J, Schmid T. Measuring the burning temperatures of anhydrite micrograins in a high-fired medieval gypsum mortar. ChemistrySelect. 2017;2:9153–6.
52. Schmid T, Jungnickel R, Dariz P. Raman band widths of anhydrite II reveal the burning history of high-fired medieval gypsum mortars. J Raman Spectrosc. 2019;50:1154–68.
53. Dariz P. Die Pietà im Kloster Marienberg. Eine Studie zu mittelalterlichem Kunststein. Zeitschrift für Kunsttechnologie und Konservierung. 2006;20:100–16.
54. Dariz P, Schmid T. Phase composition and burning history of medieval high-fired gypsum mortars studied by Raman microspectroscopy. Mater Charact. 2019;151:292–301.
55. Okrusch M, Matthes S. Mineralogie. Eine Einführung in die spezielle Mineralogie, Petrologie und Lagerstättenkunde. Berlin: Springer-Verlag; 2013.
56. Staindl A. Kurze Geologie von Südtirol. Brixen: Verlag A. Weger; 1982.
57. http://www.provinz.bz.it/hochbau/themen/1116.asp. Accessed 12 Dec 2021.
58. Götzinger M, Weber L. Industrieminerale. In: Weber L, editor. Handbuch der Lagerstätten der Erze, Industrieminerale und Energierohstoffe Österreichs. Vienna: Geologische Bundesanstalt; 1997. p. 361–8.
59. Schauberger O. Bau und Bildung der Salzlagerstätten des ostalpinen Salinars. Archiv für Lagerstättenforschung der Geologischen Bundesanstalt. 1986;7:217–54.
60. Spötl C. Sedimentologisch-fazielle Analyse tektonisierter Evaporitserien – Eine Fallstudie am Beispiel des Alpinen Haselgebirges (Permoskyth, Nördliche Kalkalpen). Geol Paläont Mitt Innsbruck. 1988;15:59–69.
61. Spötl C. The Alpine Haselgebirge Formation, Northern Calcareous Alps (Austria): Permo-Scythian evaporites in an alpine thrust system. Sediment Geol. 1989;65:113–25.
62. Paytan A, Gray E. Sulfur isotope stratigraphy. In: Gradstein F, Ogg J, Schmitz M, Ogg G, editors. The geologic time scale. Amsterdam: Elsevier; 2012. p. 167–80.
63. Claypool G, Holser W, Kaplan I, Sakai H, Zak I. The age curves of sulfur and oxygen isotopes in marine sulfate and their mutual interpretation. Chem Geol. 1980;28:199–260.
64. Denison R, Kirkland D, Evans R. Using strontium isotopes to determine the age and origin of gypsum and anhydrite beds. J Geol. 1998;106:1–17.
65. McArthur J, Howarth R, Shields G. Strontium isotope stratigraphy. In: Gradstein F, Ogg J, Schmitz M, Ogg G, editors. The geologic time scale. Amsterdam: Elsevier; 2012. p. 127–44.
66. Korte C, Kozur H, Bruckschen P, Veizer J. Strontium isotope evolution of Late Permian and Triassic seawater. Geochim Cosmochim Acta. 2003;67:47–62.
67. Prokoph A, Shields G, Veizer J. Compilation and time-series analysis of a marine carbonate $\delta^{18}O$, $\delta^{13}C$, $^{87}Sr/^{86}Sr$ and $\delta^{34}S$ database through Earth history. Earth Sci Rev. 2008;87:113–33.
68. Bernasconi S, Meier I, Wohlwend S, Brack P, Hochuli P, Bläsi H, Wortmann U, Ramseyer K. An evaporite-based high-resolution sulfur isotope record of Late Permian and Triassic seawater sulfate. Geochim Cosmochim Acta. 2017;204:331–49.
69. Worden R, Smalley P, Fallick A. Sulfur cycle in buried evaporites. Geology. 1997;25:643–6.
70. Spötl C, Pak E. A strontium and sulfur isotopic study of Permo-Triassic evaporites in the Northern Calcareous Alps. Austria Chem Geol. 1996;131:219–34.
71. Spötl C. Carbonates in Upper Permian evaporites of the Northern Calcareous Alps, Austria. Geol Rundschau. 1992;81:309–21.
72. Spötl C. Zur Altersstellung permoskythischer Gipse im Raum des östlichen Karwendelgebirges (Tirol). Geol Paläont Mitt Innsbruck. 1988;14:197–212.
73. Spötl C. Evaporitische Fazies der Reichenhaller Formation (Skyth/Anis) im Haller Salzberg (Nördliche Kalkalpen, Tirol). Jahrb Geol Bundesanst. 1988;131:153–68.
74. Spötl C. Schwefelisotopendatierungen und fazielle Entwicklung permoskythischer Anhydrite in den Salzbergbauen von Dürrnberg/Hallein und Hallstatt (Österreich). Mitt Ges Geol Bergbaustud Österr. 1988;34(35):209–29.
75. Frimmel H, Niedermayr G. Strontium isotopes in magnesites from Permian and Triassic strata, Eastern Alps. Appl Geochem. 1991;6:89–96.
76. Cortecci G, Reyes E, Berti G, Casati P. Sulfur and oxygen isotopes in Italian marine sulfates of Permian and Triassic ages. Chem Geol. 1981;34:65–79.
77. Horacek M, Brandner R, Richoz S, Povoden-Karadeniz E. Lower Triassic sulphur isotope curve of marine sulphates from the Dolomites, N-Italy. Palaeogeogr Palaeoclimatol Palaeoecol. 2010;290:65–70.
78. Ustaszewski K. Stratigraphische und strukturgeologische Untersuchungen am Ostrand der Engadiner Dolomiten (Ortler Gruppe, Südtirol). MA Thesis, Leopold-Franzens-University Innsbruck; 2000.
79. Fugger E. Die Mineralien des Herzogthumes Salzburg. Salzburg: self-published; 1878.
80. Wolf H. Das Gyps-Vorkommen von Grubach bei Golling im Kronlande Salzburg. Jahrbuch der kaiserlich-königlichen geologischen Reichsanstalt. 1873;23:47–9.
81. Schorn A, Neubauer F. Emplacement of an evaporitic mélange nappe in central Northern Calcareous Alps: evidence from the Moosegg klippe (Austria). Austrian J Earth Sci. 2011;104:22–46.
82. Schorn A, Neubauer F, Genser J, Bernroider M. The Haselgebirge evaporitic mélange in central Northern Calcareous Alps (Austria): part of the Permian to Lower Triassic rift of the Meliata ocean? Tectonophysics. 2013;583:28–48.
83. Kirchner E. Die Mineral- und Gesteinsvorkommen in den Gipslagerstätten der Lammermasse, innerhalb der Hallstattzone, Salzburg. Jahrbuch Haus Nat. 1987;10:156–67.
84. Der PW. Gipsstock von Grubach bei Kuchl. Verhandlungen der Geologischen Bundesanstalt. 1947;9:148–52.
85. Kieslinger A. Die nutzbaren Gesteine Salzburgs. Salzburg and Stuttgart: Verlag; 1964.
86. Schwendtner K. IR-spektroskopische Quantifizierungen am Gips/Anhydrit-Rohstein des Bergbaus Puchberg am Schneeberg. MA Thesis, University Vienna; 2004.
87. Ampferer O. Geologischer Führer für die Gesäuseberge. Vienna: Geologische Bundesanstalt; 1935.
88. Niedermayr G. Die Magnesite im Perm und Skyth des Drauzuges. Carinthia. 1989;II(99):391–9.
89. Bron V, Savchenko Y, Shchetnikova I, Kelareva E, Zambkovskaya G. Decomposition of magnesite during heating. Refractories. 1973;14:185–7.
90. Devasahayam S. Thermal analysis studies on the decomposition of magnesite. Int J Miner Process. 1993;37:73–88.
91. Birchal V, Rocha S, Ciminelli V. The effect of magnesite calcination conditions on magnesia hydration. Miner Eng. 2000;13:1629–33.
92. Seeley N. Magnesian and dolomite lime mortars in building conservation. J Archit Conserv. 2000;6:21–9.
93. Diekamp A. Bindemitteluntersuchungen an historischen Putzen und Mörteln aus Tirol und Südtirol. PhD Thesis, Leopold-Franzens-University Innsbruck; 2014.
94. Siedel H, Michalski S, Zier H-W. Brennen, Löschen und Erhärten von Dolomitkalken. In: Institut für Steinkonservierung (IFS), editor. Umweltbedingte Gebäudeschäden an Denkmälern durch die Verwendung von Dolomitkalkmörteln. Mainz: IFS; 2003. p. 7–10.

95. Petrascheck W, Erkan E, Hönig J. Die Gipslagerstätten der Steiermark. Mitteilungen der Abteilung für Geologie und Paläontologie und Bergbau am Landesmuseum Joanneum. 1977;38:235–45.
96. Hatle E. Die Minerale des Herzogthums Steiermark. Graz: Verlag von Leuschner & Lubensky; 1885.
97. Söding U, Dariz P. Die Schöne Madonna im Stift Marienberg und das Schöne Vesperbild in der Dompfarrkirche in Bozen. Der Schlern. 2021;95:4–35.
98. Pak E, Schauberger O. Die geologische Datierung der ostalpinen Salzlagerstätten mittels Schwefelisotopenuntersuchungen. Verhandlungen der Geologischen Bundesanstalt. 1981;2:185–92.
99. Niedermayr G, Beran A, Brandstätter F. Diagenetic type magnesites in the Permo-Scythian rocks of the Eastern Alps, Austria. In: Möller P, editor. Magnesite. Geology, mineralogy, geochemistry, formation of Mg-carbonates. Berlin: Gebrüder Borntraeger; 1989. p. 35–59.
100. Haditsch J. Die Gipslagerstätte Schildmauer bei Admont und ihre Kupfererzspuren. Archiv für Lagerstättenforschung in den Ostalpen. 1965;3:125–42.
101. Südtiroler Landesmuseum für Kultur- und Landesgeschichte Schloss Tirol, editor. Die Stuckfragmente von St. Peter. Bozen: Athesia Verlag; in press.
102. Von GW. *Ybsbrockern* und *Ybssamblern* zur Ersten Salzburger Gipswerks-Gesellschaft Christian Moldan KG. Mitteilungen der Gesellschaft für Salzburger Landeskunde. 1987;127:5–144.
103. https://geolba.maps.arcgis.com. Accessed 12 Dec 2021.
104. Hauenschild H. Das Steinguß-Materiale der Katharinen-Statue im Carolino-Augusteum in Salzburg. Mitteilungen der k.k. Zentralkommission für Erforschung und Erhaltung der kunst- und historischen Denkmale 1879;5:LXXVII–LXXVIII.
105. Hauenschild H. Das Materiale der Muttergottes-Statue des Thiemo zu St. Peter in Salzburg. Mitteilungen der k.k. Zentralkommission für Erforschung und Erhaltung der kunst- und historischen Denkmale 1879;5:CXIV–CXV.
106. Neuhardt J, Silber A. Schöne Madonnen 1350–1450. I. Bemerkungen zur Materialuntersuchung. II. Röntgenuntersuchung. Mitteilungsblatt der Museen Österreichs 1967;16:44–51.
107. Koller M. Zur Technologie und Konservierung der Vesperbilder. Österreichische Zeitschrift für Kunst und Denkmalpflege. 1970;25:188–93.
108. Perusini T, Spadea P, Casadio P. Vesperbilder del Friuli. In: Fassina V, Ott H, Zezza F, editors. The conservation of monuments in the Mediterranean basin. Venice: Soprintendenza ai beni artistici e storici di Venezia; 1994. p. 509–15.
109. Perusini T, Spadea P, Casadio P. Il Vesperbild del duomo di Gemona. Materiali e tecnologia. Studio comparato sui Vesperbilder friulani. In: Meluzzi F, editor. E vennero d'Austria e di Germania: opere e artisti d'Oltralpe a Gemona (1400–1800). Udine: Regione Autonoma Friuli-Venezia Giulia; 1995. p. 73–94.
110. Koller M, Paschinger H, Richard H. Untersuchungen zur Gußsteintechnik der Spätgotik in Mitteleuropa. Restauratorenblätter 1997/98;18:85–94.
111. Přikryl R, Racek M, Přikrylová J. Ergebnisse der Gussstein-Materialanalyse der Hallstätter Madonna in der Nationalgalerie Prag. In: Hlobil I, Mayrhofer H, Winzeler M, Chlumská Š, editors. Schöne Madonnen aus Salzburg. Gussstein um 1400. Prague: National gallery Prague; 2019. p. 72–7.

Publisher's Note